A 64×64 High-Density Redox Amplified Coulostatic Discharge-Based Biosensor Array in 180nm CMOS

Alexander Sun*, Enrique Alvarez-Fontecilla*, A. G. Venkatesh*, Eliah Aronoff-Spencer†, and Drew A. Hall*
Email: drewhall@ucsd.edu
*Department of Electrical and Computer Engineering, University of California, San Diego, La Jolla, CA, 92093, USA
†School of Medicine, University of California, San Diego, La Jolla, CA, 92093, USA

***Abstract*— This paper describes the design of a high-density 4,096-pixel electrochemical biosensor array in 180nm CMOS for biomedical applications that require multiple analyte detection from small (5µL) samples. Each pixel of the array contains an exposed 45×45µm² interdigitated micro-electrode surrounded by a ~9pL nanowell fabricated using only a standard CMOS process along with a simple electroless gold plating procedure without the need for further post processing. Directly underneath each transducer is a complete ultra-low-leakage (sub-fA) readout circuitry, which leverages the Coulostatic Discharge sensing technique and interdigitated electrode (IDE) geometry to minimize both the complexity and overall size of the array. By evaluating IDE designs with different feature sizes (2-5µm), an average maximum amplification factor of 10.5× was achieved using redox cycling coupled with the higher collection efficiency of trenches formed from opening the passivation. The array's sensor density is comparable to or better than state-of-the-art sensor arrays, all without augmenting the sensors with additional materials or structures. Using the array, detection of anti-Rubella is demonstrated as progress towards a complete vaccination panel.**

I. Introduction

High-density biosensor arrays, which consist of thousands of individually addressable miniature sensors on a single substrate, are essential for many cutting-edge biomedical applications in proteomics and genomics. One particularly interesting application is Immunosignaturing (IMS), whereby one measures the entire (or a large subset) of the humoral immune system to simultaneously detect diseases (e.g., cancer, infectious diseases, etc.) from a single droplet (5µL) of blood [1]. Hence, instead of performing several targeted tests for all the possible antibody variants associated with various diseases, which would require impracticable amounts of time, reagents, and biological samples, a single unguided assay can be run using an array of densely packed sensors functionalized to detect the antibody profile of an individual [1]. In addition, IMS technology can also be used to measure the antibodies created in the body post-vaccination, making rapid and comprehensive verification of immunization possible.

However, IMS as well the other aforementioned applications traditionally use optical detection requiring complex imaging tools too bulky and impractical to bring to the point-of-care (POC), where measurements need to be made in remote areas away from the resources of centralized labs. To address this issue, this work aims to miniaturize and convert the assay to an electrochemical format enabling portable, POC IMS testing. While electrochemical detection is known to improve the size, cost, and scalability of biosensors, most high-density array implementations still require a full potentiostat [2]–[6] with a very sensitive transimpedance amplifier (TIA) or current conveyor to measure the minute signals associated with microelectrodes (Fig. 1a). Furthermore, even if one could build such a high performance potentiostat, scanning a large array would require either time domain multiplexing or having multiple copies, which would be area prohibitive. As the sensor density increases, the constraints of both the circuit area of each pixel and required sensitivity become increasingly difficult to satisfy simultaneously.

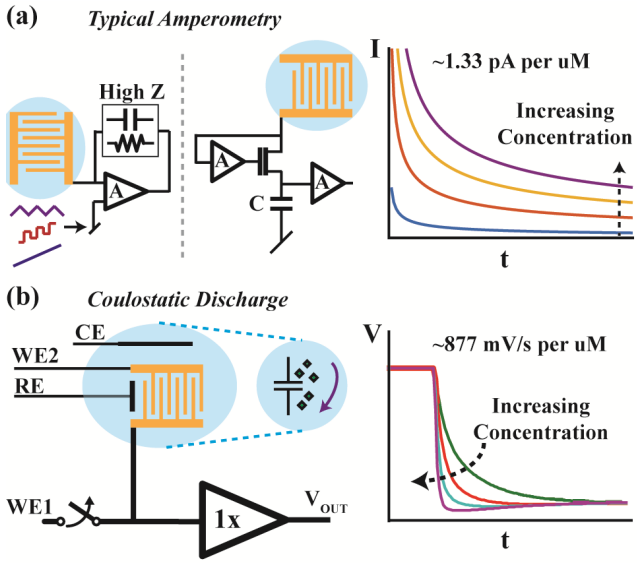

Fig. 1: (a) Typical measurement circuits for amperometric techniques in high-density arrays (left) and simulated chronoamperometry plots for µM range concentrations (right). (b) This work's Coulostatic Discharge measurement circuit (left) and calculated discharge rate curves for the same sensor size and concentrations (right).

To solve these issues, many potentiostat-based arrays either have specially fabricated sensors to increase sensitivity or move parts of the measurement circuitry outside of the array to decrease the pixel size. However, since neither method addresses the fundamental difficulty of measuring small current, in this paper, we describe the design and validation of an integrated high-density array biosensor that instead leverages a little-used electrochemical detection method, Coulostatic Discharge (Fig. 1b), to significantly reduce the

This work was partially supported by Intel Labs through SRC and the UCSD Medical Devices and Systems (MDS) initiative.

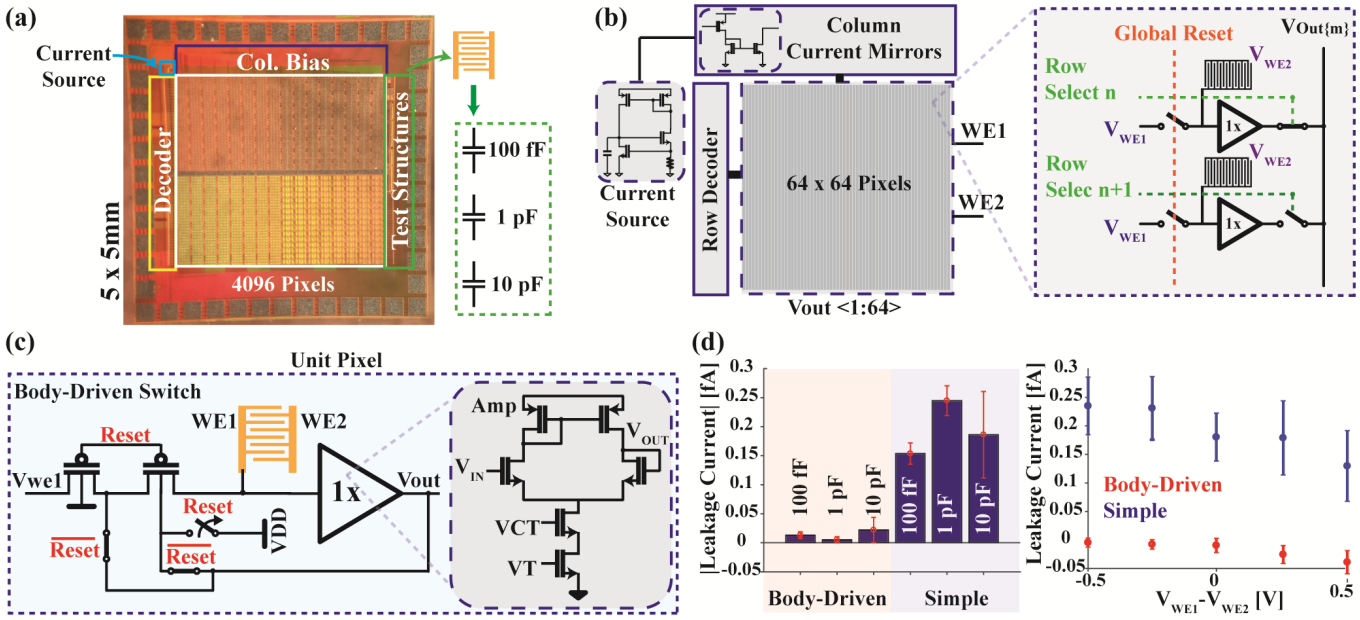

Fig. 2: (a) Photograph of the high-density array IC with the various blocks annotated. The test structures include known capacitors connected to either a body-driven or simple switch. (b) Block diagram of the overall architecture of chip and (c) schematic of the body-driven switch. (d) Average leakage measurement results from each of the test structures with 0.5 V applied across each (left). The average leakage of all the test structures at different sensor voltages.

complexity and size of the measurement circuitry for each pixel. As illustrated in Fig. 1, the transduced signal from this technique is a transient voltage, instead of a current, thereby decreasing the area and power consumption of the readout circuitry for each sensor since a large ~1V/s/µM discharge rate is simpler to measure than ~1pA/µM. Hence, this technique along with electrochemical amplification from interdigitated electrodes (IDEs), efficient utilization of the inherent double layer capacitance, and inherent trench-gap structure allows one to pack all the sensors and circuitry densely enough for high-density array applications by only using the capabilities of a standard CMOS process without additional fabrication steps.

II. Electrochemical Measurement Circuitry

A. Coulostatic Discharge-Based Detection Method

In the electrochemical technique known as the Coulostatic Discharge [7]–[9], the sensor itself is used to convert the miniscule current into an easily digitized voltage. Hence, instead of applying a continuous potential waveform to an electrochemical sensor and measuring the current response, as is the case with a typical potentiostat, a potential is applied only briefly allowing a build-up of charge to form at the interface between the electrode and the ionic solution, also known as the double layer capacitance, C_{dl}, as shown in Fig. 1. After the source supplying the potential to the electrode is disconnected, C_{dl} is discharged through the electrochemical cell decreasing the voltage of the electrode at a rate related to the concentration of the electrochemically active species present. A signal on the order of ~100mV is measured with readout circuitry consisting of a buffer to sample the discharge voltage and an ultra-low leakage switch to reduce errors.

It is worth noting that the presence of C_{dl} here obviates the need for an on-chip discharge capacitor for each pixel since the ionic concentration range and electrode area used form a large enough capacitance (~10-100pF) that a separate one is unnecessary, thus saving space. Furthermore, using C_{dl}, which scales directly with area, creates the added benefit that as the electrode area becomes smaller and the current flowing from it decreases, C_{dl} also reduces maintaining the rates of discharge at the same level regardless of the surface area.

B. Low-Leakage Switch Array Architecture

Architecturally, the chip (Fig. 2a) is arranged like an imager with a shared working electrode (WE2), a row decoder, and column parallel readout (Fig. 2b). Each pixel requires only a buffer, both to provide isolation and to readout the voltage of the electrode, and an ultra-low leakage switch. A body-driven switch (Fig. 2c) [10], which reuses the output buffer to drive the body of the transistor, was designed to minimize the leakage at the working electrode. Furthermore, an additional switch connecting the output buffer to the node between the two PMOS transistors was added to remove the voltage drop over the PMOS adjacent to the working electrode further reducing the leakage. The buffer is implemented using a conventional five transistor differential structure with 42.8dB gain and 26kHz unity gain bandwidth. It is optimized for low $1/f$ noise given the limited area. The entire circuitry fits underneath a 45×45µm^2 sensor using three metal layers since the sensor is fabricated using the upper metal layer. A network of current mirrors distributes the reference current generated by the on-chip current source down each column to a set of local mirrors. Each of these local current mirrors is shared among a 4×4 subset of the array to bias the buffers.

Using test structures with MIM capacitors in place of the sensors (Fig. 2a), the body-driven switch leakage was measured to be 0.013fA compared to a simple PMOS switch which had 0.195fA (Fig. 2d). The body-driven switch had

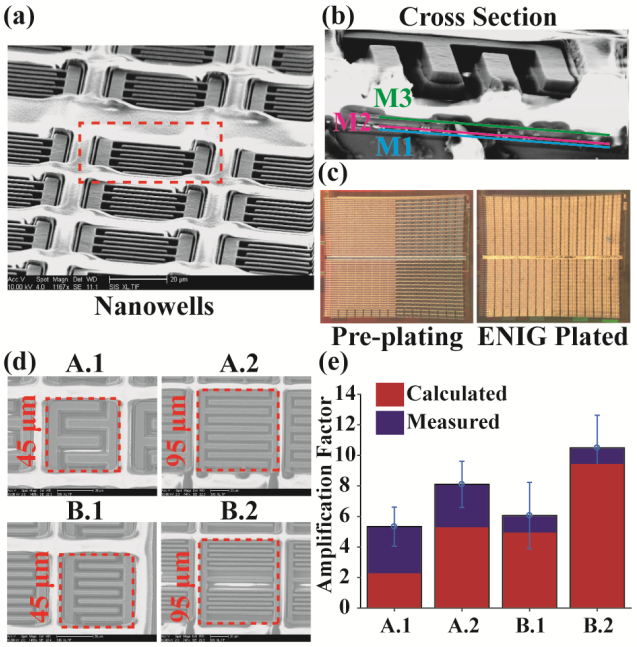

Fig. 3: (a) SEM of the chip angled to show the nanowell structure. (b) SEM of the chip cross-section with the metal layers annotated. (c) Photograph of the chip before and after ENIG plating. (d) SEM of each electrode design. (e) Calculated and measured maximum amplification factor using Coulostatic Discharge.

better performance across the entire voltage range. The 4,096 sensor chip consumes a max of 95mW from a 2.5V supply.

III. Sensor Fabrication

The microelectrode sensor consists of two interdigitated electrodes, designed to amplify the signal using redox cycling, fabricated using the top metal layer. Redox cycling is the effect when a reversible redox pair repeatedly diffuses between two differently biased electrodes transferring electrons through reduction and oxidation at the two electrodes. Hence, a single redox molecule can contribute multiple times to the overall current. During the fabrication process, the passivation directly above each sensor was removed exposing this structure and creating nanowells (Fig. 3a) to isolate the sensors and contain the redox active molecules generated during the assay. Since the passivation was opened across the entire IDE including the gaps, 3D trenches between the two electrodes were created that increase collection efficiency by trapping the redox molecules and further amplifying the signal (Fig. 3b). For electrochemical compatibility, a simple industry standard electroless nickel immersion gold (ENIG) plating process was used to plate the exposed top metal aluminum electrodes (Fig. 3c).

Four different electrode designs were fabricated (Fig. 3d) with finger and gap widths of 5µm and 5µm for electrodes A.1 and A.2 and 2µm and 3µm for B.1 and B.2. In PBS, the C_{dl} of these designs range from 24-180pF. With this geometry, an approximate amplification factor was calculated to be 2.25×, 5.27×, 4.93×, and 9.41× [11]. Using Ferro/Ferricyanide, external reference and counter electrodes, and Coulostatic Discharge both in single working electrode and dual working

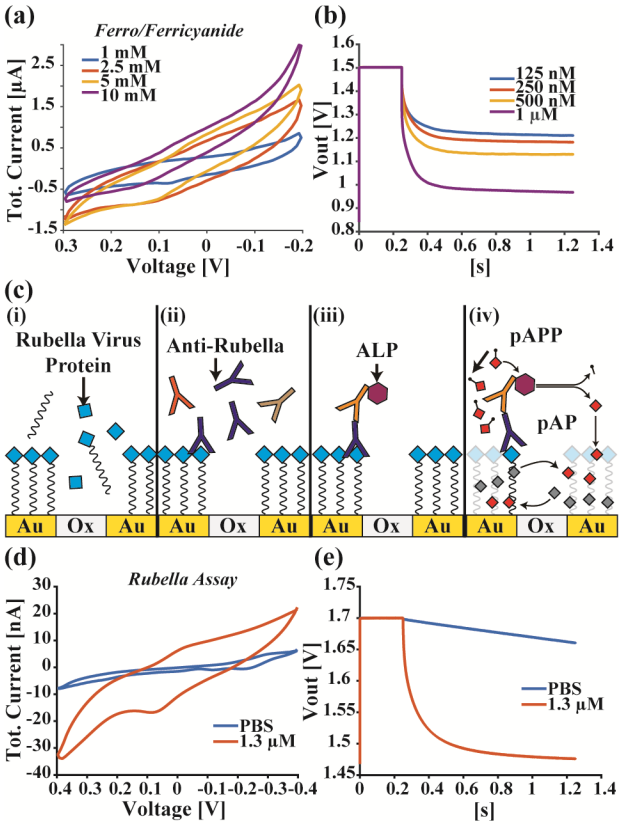

Fig. 4: (a) CV and (b) Discharge measurements of combined working electrodes with various concentrations of Ferro/Ferricyanide. (c) Illustrated steps in Anti-Rubella antibody assay. (d) CV assay results of combined working electrodes and (e) discharge measurements for a single IDE for both PBS and 1.3µM anti-Rubella.

electrode modes, the amplification factor was measured. The average amplification factors for each design are 5.33×, 8.1×, 6.06×, and 10.5×, respectively (Fig. 3e). These measured values are slightly larger than the theoretical values most likely due to the 3D trench and nanowell structures. Also, IDEs with the same gap and finger widths but greater number of fingers have higher amplification. Smaller gap size also increases the redox cycling.

IV. Electrochemical Verification and Assay

After cleaning the chip by sonicating in isopropyl alcohol, the chip was mounted in a socket designed to create a ~10µL well over the sensors. External Ag/AgCl and Pt electrodes were dipped into this well to form the reference and counter electrodes. Fig. 4a-b demonstrates that the array can measure Ferro/Ferricyanide, a standard reversible redox pair, using both cyclic voltammetry (CV) and Coulostatic Discharge techniques. While CV measurements could only be made by combining all the working electrodes together, the Coulostatic Discharge measurements were done individually with the working electrodes biased at 0.2V and -0.2V (vs. Ag/AgCl).

To demonstrate a bioassay (Fig. 4c), Rubella virus capsid protein was dropcasted on the surface of the gold sensor array using Traut's Reagent and blocked with bovine serum albumin (BSA). Mouse anti-Rubella antibodies were subsequently

TABLE I
COMPARISON WITH STATE-OF-THE-ART INTEGRATED ELECTROCHEMICAL BIOSENSOR ARRAYS

REF.	HASSIBI [2]	MANICKAM [3]	KIM [4]	ROTHE [5]	HALL [10]	NASRI [6]	THIS WORK
Technology (µm)	0.18	0.35	0.5	0.35	0.032	0.065	***0.18***
Num. Pixels	50	100	100	1,024	8,192	4	***4,096***
Sensor Density [#/mm^2]	52.1	69.4	1,046	100	50,000	22.2	***400***
Total Density [#/mm^2]	11.90	25.00	11.11	28.44	327.68	0.44	***163.84***
Electrode Area [µm^2]	3,600	1,600	225	491	1	5,000	***2,025***
Pixel Area [µm^2]	19,200	10,000	745	10,000	20	45,000	***2,500***
Devices Per Pixel	301	34	>9*	21**	3	37	***12***
Post Processing?	NO	NO	YES	YES	YES	YES	***NO***
Dual Electrode?	YES	NO	NO	NO	YES	NO	***YES***
Technique	MULTIPLE	EIS	CA	AMP.	CD	FSCV	***CD***

EIS – Electrochemical Impedance Spectroscopy, CA – Chronoamperometry, Amp. – Amperometry, CD – Coulostatic Discharge, FSCV – Fast Scan Cyclic Voltammetry
* Part of the measurement circuitry is located outside of the pixel and a 50fF capacitor and buffer circuit were not included in the device count.
** All the measurement circuitry is located outside of the pixel. This is a per row device number.

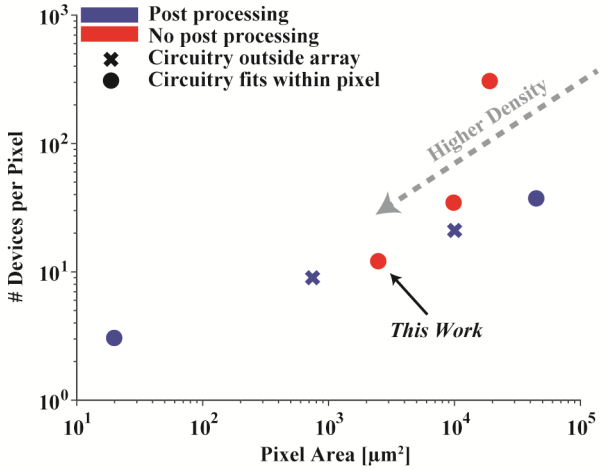

Fig. 5: Plot comparing the pixel areas and number of devices per pixel of high-density electrode arrays summarized in Table I.

added and incubated for 1 hour. Rabbit anti-mouse secondary antibodies linked with the alkaline phosphatase (ALP) enzyme were used as the secondary. Lastly, the p-aminophenyl phosphate (pAPP) substrate was added and allowed to incubate for 20 min. The ALP enzyme reacts with the pAPP substrate producing p-aminophenol (pAP), an electrochemically active molecule that shuttles electrons between the two fingers of the sensor. Fig. 4c-d shows measurement results for both CV and Coulostatic Discharge successfully detecting the presence of anti-Rubella antibodies over a blank control.

V. DISCUSSION

Table I compares this work to other integrated electrochemical biosensor arrays, and Fig. 5 plots their pixel areas and number of devices per pixel with different markers to signify those that have special post processing and/or have measurement circuitry external to the array. Due to redox cycling, this work achieves a relatively small pixel area and high sensor density (400 pixels/mm^2) without any post-processing, which others do to increase sensitivity. While augmenting sensors with additional structures and materials is effective, it requires complex fabrication steps that are much more difficult and expensive to produce and scale than an array built purely with a standard process. To the best of our knowledge, this work is the highest density amperometric biosensor array that does not require additional post-processing steps. Furthermore, Coulostatic Discharge greatly decreases the number of devices required in the measurement circuitry (~12), allowing all the circuit to reside completely within the area of a pixel. In fact, the two arrays based on Coulostatic Discharge [10] have the lowest number of devices that fit completely within a pixel. Hence, rather than occupying a considerable amount of area with circuit blocks external to the array, this work makes efficient use of the chip area as illustrated by the total density calculation in Table I.

REFERENCES

[1] J. B. Legutki, Z.-G. Zhao, M. Greving, N. Woodbury, S. A. Johnston, and P. Stafford, "Scalable high-density peptide arrays for comprehensive health monitoring," *Nat. Commun.*, vol. 5, Sep. 2014.

[2] A. Hassibi and T. H. Lee, "A programmable electrochemical biosensor array in 0.18 µm standard CMOS," in 2005 ISSCC, 2005, p. 564–617 Vol. 1.

[3] A. Manickam, A. Chevalier, M. McDermott, A. D. Ellington, and A. Hassibi, "A CMOS electrochemical impedance spectroscopy biosensor array for label-free biomolecular detection," in 2010 ISSCC, 2010, pp. 130–131.

[4] B. N. Kim, A. D. Herbst, S. J. Kim, B. A. Minch, and M. Lindau, "Parallel recording of neurotransmitters release from chromaffin cells using a 10×10 CMOS IC potentiostat array with on-chip working electrodes," *Biosens. Bioelectron.*, vol. 41, pp. 736–744, Mar. 2013.

[5] J. Rothe, O. Frey, A. Stettler, Y. Chen, and A. Hierlemann, "Fully Integrated CMOS Microsystem for Electrochemical Measurements on 32 × 32 Working Electrodes at 90 Frames Per Second," *Anal. Chem.*, vol. 86, no. 13, pp. 6425–6432, Jul. 2014.

[6] B. Nasri et al., "15.7 Heterogeneous integrated CMOS-graphene sensor array for dopamine detection," in 2017 ISSCC, 2017, pp. 268–269.

[7] X. Zhu, J.-W. Choi, and C. H. Ahn, "A new dynamic electrochemical transduction mechanism for interdigitated array microelectrodes," *Lab. Chip*, vol. 4, no. 6, pp. 581–587, Nov. 2004.

[8] A. Sun, A. Au, A. G. Venkatesh, V. Gilja, and D. A. Hall, "A scalable high-density electrochemical biosensor array for parallelized point-of-care diagnostics," in 2015 BioCAS, 2015, pp. 1–4.

[4] P. Delahay, "Coulostatic Method for The Kinetic Study of Fast Electrode Processes. I. Theory," J. Phys. Chem., vol. 66, no. 11, pp. 2204–2207, Nov. 1962.

[10] D. A. Hall et al., "16.1 A nanogap transducer array on 32nm CMOS for electrochemical DNA sequencing," in 2016 ISSCC, 2016, pp. 288–289.

[11] V. a. T. Dam, W. Olthuis, and A. van den Berg, "Redox cycling with facing interdigitated array electrodes as a method for selective detection of redox species," *Analyst*, vol. 132, no. 4, pp. 365–370, Mar. 2007.